Evaluation of Analog Encoding for Multi-User Wireless Transmission of Still Images

Jose Balsa, Óscar Fresnedo, Tomás Domínguez-Bolaño, José A. García-Naya, and Luis Castedo
CITIC, Universidade da Coruña (University of A Coruna), SPAIN
{j.balsa, oscar.fresnedo, tomas.bolano, jagarcia, luis}@udc.es

***Abstract*—In this paper, we present an analog system to transmit still images over multiuser wireless channels and an empirical comparison with a representative digital scheme. The tests were carried out considering a multiple access channel (MAC) where two single-antenna users transmit their images to a two-antennas centralized receiver. The analog system encodes the source images using analog joint source-channel coding (JSCC) mappings and the resulting symbols are packed into an orthogonal frequency-division multiplexing (OFDM) frame. The quality of the analog received image is evaluated with the structural similarity (SSIM) and a digital image with the same quality is generated, which is encoded into an OFDM frame and transmitted over the same channel estimated as the analog one. The aim of this work is to compare the transmission times of the two systems and evaluate the suitability of the analog encoding techniques for the transmission of still images.**

I. Introduction

The design of communication systems is traditionally based on the digital encoding of the source information prior to be transmitted. When the nature of the source information is analog, the input signal is first sampled and quantized to obtain a set of representative discrete-time discrete-amplitude symbols. A source encoder is then employed to produce an appropriate binary representation of the source symbols by removing the existing redundancy. Finally, a channel encoder is used to protect the information bits against potential channel distortions. This design strategy is known as the source-channel separation principle, and it simplifies the optimization of the encoding operations besides being able to provide the optimal performance for the lossless and lossy compression of analog information in a wide range of communication scenarios [1]–[3]. However, its theoretical optimality is based on the use of large block sizes at both encoders, thus resulting in a large complexity and communication delay. This strategy has also some issues related to its practical implementation such as the need of having accurate channel information to adjust the digital encoders and the impact of reducing the block size on the overall performance [4], [5]. Hence, these problems make this approach unsuitable for real-time communications over time-varying channels with a low coherence time. In addition, it is no longer optimal when we consider multiuser or network communications [6]–[9].

In this kind of communication scenarios, an appealing alternative consists in considering the analog joint source-channel coding (JSCC) of the source information where the discrete-time continuous-amplitude symbols obtained after the sampling operation are directly encoded into the channel symbols to be transmitted. The encoding operation is based on the use of continuous geometric curves defining the relationship between the points on the source space and their corresponding points on the channel space [10], [11]. Although the optimization of the joint encoder is more involved, analog JSCC-based schemes present low computational cost and negligible delay, high transmission rates, simple adaptation to the channel variations by adjusting a few parameters of the mapping function, and graceful degradation in case of inaccurate channel information. This latter property is particularly attractive when broadcasting the same information to multiple receivers with different channel qualities, or when transmitting to a single receiver over an unknown fading channel. These schemes also provide a competitive performance (even better) with respect to practical digital systems when transmitting Gaussian sources in different scenarios such as additive white Gaussian noise (AWGN) channels [12], fading multiple-input and multiple-output (MIMO) channels [13] and network communications [14]. All these features make analog JSCC to be a promising candidate for the coming communication systems where there are severe constraints on the delay and/or the transmission rates.

In this paper, we address the design and optimization of an analog JSCC scheme for a multiuser scenario where two users transmit still images to a common receiver equipped with several antennas. We also consider that the analog encoded symbols corresponding to the user images are modulated using orthogonal frequency-division multiplexing (OFDM) before being transmitted to the receiver over fading channels. The performance of the proposed analog JSCC scheme is assessed in the considered scenario and compared to that of a digital system based on Joint Photographic Experts Group (JPEG).

II. System Model

We consider the multiuser transmission of still images over uncorrelated Rayleigh channels. More specifically, we consider a multiple access channel (MAC) where two single-antenna users transmit their images to a two-antennas centralized receiver. Source images are encoded using low complexity zero-delay analog JSCC mappings and the performance of this scheme will be compared to that of a digital one employing the JPEG standard. For simplicity, we will only consider gray-scale images.

978-9-0827-9703-9/19/$31.00

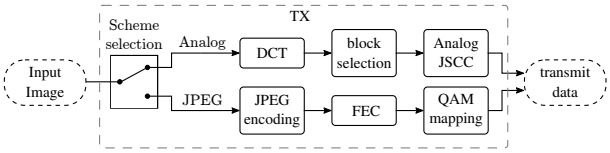

Fig. 1. Transmitter diagram.

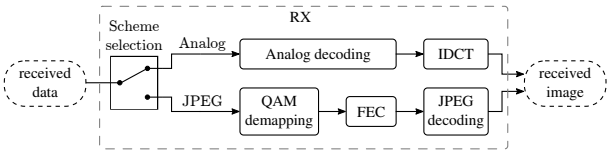

Fig. 2. Receiver diagram.

Figs. 1 and 2 show the diagrams of the transmitter and receiver, respectively, including the analog and the digital schemes. The transmitter and receiver of both schemes are detailed in Sections III and IV, respectively. The transmitter shown in Fig. 1 receives a gray-scale image as an input, performs an analog or digital processing depending on the considered scheme and returns a vector of complex-valued data symbols to be transmitted. Analogously, the receiver in Fig. 2 receives a vector of complex-valued symbols and returns the received image after the corresponding decoding operation. The diagram of the complete system is shown in Fig. 3.

Each user encodes its data into an OFDM frame and both frames are transmitted simultaneously. Note that we consider that the transmit symbols returned by the transmitter (see Fig. 1) are normalized, i.e., their mean power is one. Apart from the synchronous transmission requirement, we consider that both users do not cooperate with each other and their source images are also not correlated.

Regarding the OFDM modulation, we consider a setup similar to that of the $10\,\mathrm{MHz}$ profile of LTE, using 600 subcarriers (i.e., we use 600 points, excluding the DC one, of an inverse fast Fourier transform (IFFT) of 1024 points), a subcarrier spacing of $15\,\mathrm{kHz}$, a cyclic prefix (CP) length of $4.69\,\mu\mathrm{s}$, and a pilot spacing of 6 symbols in frequency and 4 symbols in time. The two users use an orthogonal pilot sequence in which each user transmits zeros in the time-frequency positions of the pilots of the other user.

The OFDM signals are transmitted through a fading channel and AWGN is added. The channel response is modeled as a 2×2 matrix whose components are obtained from a complex-valued standard Gaussian distribution, thus obtaining a flat Rayleigh channel with uncorrelated coefficients. Then, a noise component is added to obtain a desired mean symbol signal-to-noise ratio (SNR) (i.e., the SNR of the symbols after the OFDM demodulator). Due to the fact that the transmit symbols are normalized and that the channel coefficients are obtained from a complex-valued standard Gaussian distribution, the noise power is simply obtained as $\sigma^2 = 2/\mathrm{SNR}$ for a given SNR, where the 2 in the numerator is the number of users.

Once the two signals are received, OFDM demodulation is performed, and then the four channels of the link are estimated by means of the pilots. Using the estimated channels, the received symbols are equalized to decouple the data streams corresponding to each user. For both the channel estimation and equalization procedures minimum mean square error (MMSE) algorithms are employed. Finally, the equalized symbols are passed to the corresponding receiver (see Fig. 2) which computes an estimate of the transmitted symbols and reconstructs the received image from those estimates.

III. Analog Scheme

The analog transmitter will transform an input gray-scale image into a vector of analog coefficients. The first step is to divide the image into blocks of size 8×8 pixels. A discrete cosine transform (DCT) is applied to each block to convert them to the frequency domain. Following the same idea of the JPEG standard, we assume that the coefficients corresponding to the lower frequencies capture more information about the source image, and thus are more important than coefficients of higher frequencies. Therefore, the obtained coefficients from the DCT are arranged into a vector from the lower to the higher frequencies following a zig-zag pattern.

The following step is to apply analog JSCC mappings to the frequency-domain coefficients. As commented in the introduction, it is important to first remove part of the image redundancy to lower the amount of data to be encoded with the analog mappings. Since we consider that the importance of these coefficients depends on their frequency (i.e., their position in the vector), we split the vector of DCT coefficients into n_b variable-size vectors, $\boldsymbol{s}_i = [s_{i,1}, \ldots, s_{i,N_i}]$, $i = 1, \ldots, n_b$, where N_i is the number of elements in the vector $\boldsymbol{s}_i$. This block division allows us to implement a simple compression operation by selecting only a subset of vectors to be encoded while disregarding the remaining ones. This simple scheme has also the advantage that the selection pattern is known by both the transmitters and the receiver, and hence it is not required to transmit additional metadata.

In this paper, we will consider a block division with $n_b = 4$ vectors and sizes $N_1 = 1$, $N_2 = 3$, $N_3 = 12$, and $N_4 = 48$. Since we are assuming that the higher frequency coefficients carry less visual information, we can disregard them without impacting significantly on the image quality. Therefore, a reasonable strategy would be to transmit only the first n_c vectors, disregarding the rest. In this work we design the analog JSCC scheme considering two different values for n_c, namely $n_c = 2$ and $n_c = 3$.

These n_c vectors of coefficients are encoded with analog JSCC mappings, i.e.,

$$\boldsymbol{x}_i = f_i(\boldsymbol{s}_i), \quad i = 1, \ldots, n_c, \tag{1}$$

where $f_i(\cdot)$ is a mapping function applied individually to the i-th vector of coefficients. We focus on two particular mapping functions: linear coding, and spherical codes based on the exponentially chirped modulation [15]. The first scheme simply sends a scaled version of the input symbols, whereas the latter one is an expansion code used to increase the protection level of the input symbols. In general, the selected vectors are encoded using the linear mapping, although the

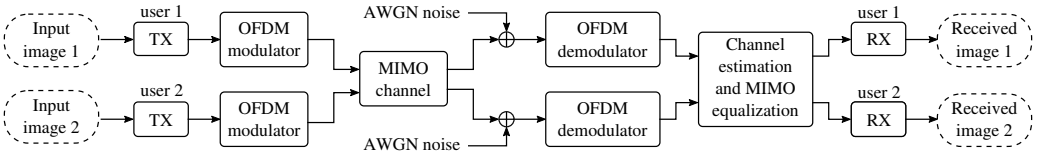

Fig. 3. System model diagram.

TABLE I
CONSIDERED ANALOG DECODING STRATEGIES.

SNR range	Analog decoding strategies for the received vectors			
	$\boldsymbol{s}_1$	$\boldsymbol{s}_2$	$\boldsymbol{s}_3$	$\boldsymbol{s}_4$
< 6 dB	Linear MMSE	Linear MMSE	Linear MMSE or refill with zeros	refill with zeros
6 dB to 11 dB	ML			
11 dB to 16 dB	ML			
> 16 dB	Linear MMSE			

mapping function applied to the vector $\boldsymbol{s}_1$ will depend on the link SNR.

Note that the vector $\boldsymbol{s}_1$ only contains the coefficients corresponding to the DC component of the pixel blocks, hence we consider that it has the most valuable visual information. As the SNR becomes lower, it is necessary to introduce extra redundancy to minimize the visual degradation of the received image. Therefore, we propose an encoding scheme considering four different mappings for $\boldsymbol{s}_1$ with four different protection levels depending on the SNR. For SNR values lower than 6 dB, we use a repetition code with 4 repetitions. This strategy is the most appropriated in the low SNR regime because the non-linearity nature of the spherical codes could lead to visual artifacts. For SNR values between 6 and 11 dB we use an spherical code with an expansion factor $L = 4$. For SNR values between 11 and 16 dB we consider an spherical code with an expansion factor $L = 2$. Finally, for SNR values greater than 16 dB we employ linear transmission because the channel quality is enough. The other $n_c - 1$ selected vectors are always transmitted with the linear mapping because their impact on the visual quality of the image is lower.

At reception, the analog decoder obtains an estimate of the coefficients of the n_c encoded vectors from the equalized symbols. Table I shows the method used to recover the coefficients corresponding to each vector. Two different strategies are considered for the estimation of the first vector depending on the type of mapping considered in the encoding operation. On the one hand, linear MMSE estimation is appropriate for the cases of a linear repetition code and a linear mapping. On the other, a low-complexity decoding based on maximum likelihood (ML) is applied to estimate the coefficients encoded with the spherical codes. Note that the coefficients corresponding to the disregarded vectors are set to zero.

After the decoding operation, the estimated coefficients are used to reconstruct the received image by means of the inverse of the DCT, and the quality of the received image is computed using the structural similarity (SSIM) metric.

Fig. 4. Transmit images from the left-hand side: "Lena" and "Gold Hill".

IV. DIGITAL SCHEME AND EVALUATION METHODOLOGY

The digital transmitter, as shown in Fig. 1, transforms an input gray-scale image into a vector of quadrature amplitude modulation (QAM) symbols. This scheme follows the traditional approach of source-channel separation coding. In this case, the source coding operation is performed with the standard JPEG encoder, which applies a lossy compression to the input image. The level of compression can be adjusted by changing the quality parameter of the JPEG encoder. For the channel coding, we use a turbo-coder as defined by the Long-Term Evolution (LTE) standard. For the QAM modulation orders and coding rates, we use the ones specified in the LTE standard [16, Table 7.2.3-1]. Each possible combination is identified by a channel quality indicator (CQI) index, ranging from 1 (the lowest modulation order and coding rate) to 15 (the highest modulation order and coding rate). The receiver, as shown in Fig. 2, transforms the input symbols into the received image by undoing the steps carried out by the transmitter.

We compare the analog and digital systems by assessing the transmission time for some test images. In this paper, we consider the two images shown in Fig. 4, each one of 512×512 pixels. To perform the comparison, the two users first transmit an image with the analog JSCC system for a given channel realization and a given SNR. At the analog receiver, the received images are decoupled and recovered for both users, and their SSIM indexes are computed. Next, the images are transmitted with the digital system using the same channel realization and SNR. For this transmission, we adjust the quality parameter of the JPEG encoder for each user so that the SSIM of the resulting image is as close as possible to the SSIM previously calculated for the corresponding received analog image. For the CQI index (i.e., the modulation and coding rate), we use the optimum one, i.e., the highest one such that the received bit stream is decoded without errors. For simplicity, we employ the same CQI value for both users and for a given transmission. Finally, the transmission times are calculated for each image as the length in seconds of

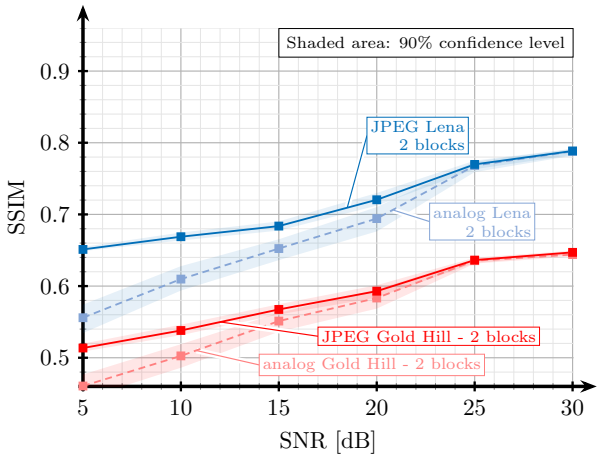

Fig. 5. SSIM comparison in the two-blocks scenario ($\boldsymbol{s}_1$ and $\boldsymbol{s}_2$ are transmitted).

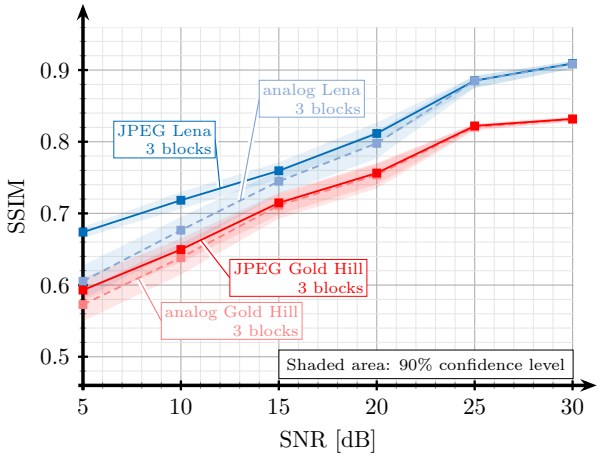

Fig. 6. SSIM comparison in the three-blocks scenario ($\boldsymbol{s}_1$, $\boldsymbol{s}_2$ and $\boldsymbol{s}_3$ are transmitted).

the transmitted OFDM frames. Note that the analog scheme generates for the two images the same amount of data, thus the transmission time will be the same. However, the data generated by the JPEG encoder depends not only on the image quality but also on the image itself, so the transmission time may be different for both images. Therefore, to evaluate the digital system we transmit the images cyclically. Hence, both users are always transmitting data (and interfering each other).

V. Results

We show in Figs. 5 and 6 the mean SSIM values for the analog and digital systems versus the SNR. Fig. 5 shows the results for the case in which the blocks $\boldsymbol{s}_1$ and $\boldsymbol{s}_2$ are transmitted, whereas Fig. 6 considers also the transmission of $\boldsymbol{s}_3$. As expected, higher SSIM values are in general obtained for the case of transmitting $\boldsymbol{s}_3$, although this gain is less significant in the low SNR regime. On the other hand, the SSIM increases with the SNR in a quasi-linear way for both configurations. Note that, as explained in Section IV, for a given received analog image, a digital image is generated with an SSIM value as close as possible to that of the received analog image. However, in the digital case, the SSIM exhibits

Fig. 7. SSIM visual analysis. Left: analog received image for $n_c = 2$ with 0.70 SSIM. Right: JPEG image with 0.72 SSIM.

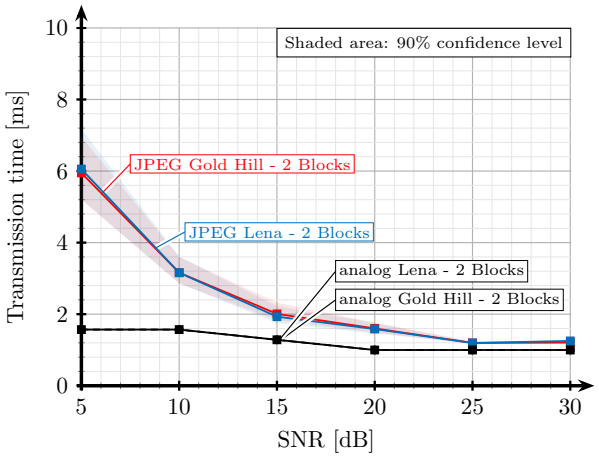

Fig. 8. Transmission time comparison in the two-blocks scenario.

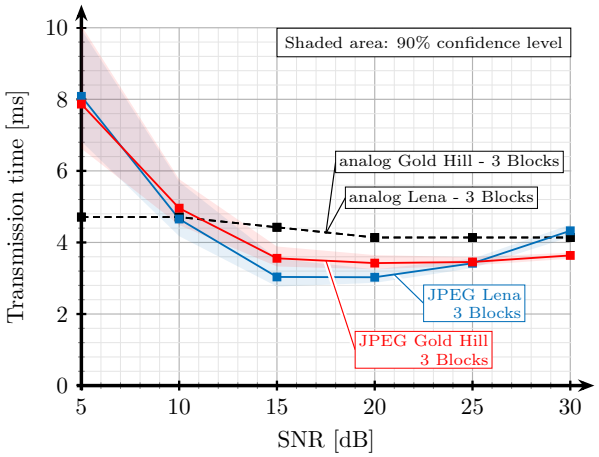

Fig. 9. Transmission time comparison in the three-blocks scenario.

a lower bound corresponding to the lowest value of the quality parameter of the JPEG encoder. For the analog system, since the received images are affected by additive noise, the SSIM index may be lower. This is the cause of the gaps between the mean SSIM values for the analog and digital schemes for low SNR values, which are shown in Figs. 5 and 6.

The SSIM is an adequate metric considered for still images, but it does not necessarily capture the visual quality of the resulting images in an accurate way. In Fig. 7 we show an example where we compare an analog image for $n_c = 2$ with an SSIM of 0.70, and a JPEG compressed image with an SSIM of 0.72. Although the SSIM of both images is similar, it can be

TABLE II
DIGITAL SYSTEM BEHAVIOR. JPEG "LENA" IMAGE FOR THE THREE-BLOCKS SCENARIO.

SNR (dB)	Image quality (SSIM)	Transmission time (ms)	Mean CQI	Source bits (kbit)
5	0.67	8.08	5.27	37.9
10	0.72	4.66	7.45	45.32
15	0.76	3.04	10.30	53.99
20	0.81	3.03	12.13	79.77
25	0.89	3.42	14.63	125.51
30	0.91	4.33	14.83	159.56

seen that the analog one, although distorted by noise, preserves the details better than the digital one.

Figs. 8 and 9 show the mean transmission time per image. Note that, in the proposed analog system, the same mapping functions are applied to $\boldsymbol{s}_2$ and $\boldsymbol{s}_3$, but for $\boldsymbol{s}_1$ a different mapping function is applied depending on the SNR values. Therefore, the transmission time of the analog system depends on the SNR as shown in Figs. 8 and 9, whereas the transmission time of the digital system depends on the image quality and the CQI index used. As observed in Fig. 8, the time required to transmit the two images with the analog scheme is shorter for the considered SNR range. In the digital case, the transmission time for both images is almost the same. This time decreases fast with the SNR value, up to $25\,\mathrm{dB}$, but from this value the transmission time does not improve.

Regarding Fig. 9, the digital scheme is able to provide a shorter transmission time for some SNR values, but the analog JSCC scheme is still competitive in this scenario. Again, the transmission times of the analog system are similar for the whole SNR range. In the digital case, these times lower with the SNR up to a value of $15\,\mathrm{dB}$, but for greater values of SNR the performance no longer improves, and even worsens for the case of the "Lena" image. This effect is caused because the mean CQI saturates at its highest possible value, but the source bits keep increasing with the SNR, as shown in Table II.

VI. CONCLUSIONS

In this work, we presented a robust multiuser analog JSCC scheme to transmit still images. The system is based on splitting the vector of DCT coefficients into a fixed number of blocks. Transmitting $n_c = 2$ blocks, as opposed to the $n_c = 3$ blocks case, results in less transmitted data at the expense of reducing slightly the quality of the image.

We performed simulations considering Rayleigh channels with two users transmitting simultaneously, each one with one antenna, and a receiver with two antennas. The proposed system was compared to a digital system using the JPEG encoder as the source code and a turbo-encoder as the channel code. The comparison methodology consisted in transmitting an image with the analog system through a given channel realization and then generate and transmit a digital image with a quality (in terms of SSIM) as close as possible to that of the analog received image. Results showed that when using $n_c = 2$ blocks, the transmission times for the analog system are shorter than those required by the digital system for the considered SNR range. For the case of $n_c = 3$, the analog system performed better for low SNR values (less than $10\,\mathrm{dB}$). However, for larger values of SNR, the improvement exhibited by the digital system is not substantial. Note that for the digital system we are not taking into account the retransmissions that would occur on a real system, which would impact on the delay and the jitter of the system. Therefore, the proposed analog system can be a good candidate for low-delay applications.

ACKNOWLEDGMENT

This work has been funded by the Xunta de Galicia (ED431C 2016-045, ED431G/01), the Agencia Estatal de Investigacin of Spain (TEC2016-75067-C4-1-R) and ERDF funds of the EU (AEI/FEDER, UE).

REFERENCES

[1] C. E. Shannon, "A mathematical theory of communication," *The Bell System Technical Journal*, vol. 7, pp. 379–423, 1948.
[2] T. Berger, *Rate Distortion Theory: A Mathematical Basis for Data Compression*. Englewood Cliffs, 1971.
[3] S. Vembu, S. Verdu, and Y. Steinberg, "The source-channel separation theorem revisited," *IEEE Trans. Inf. Theory*, vol. 41, no. 1, pp. 44–54, Jan. 1995.
[4] M. M. Shanechi, R. Porat, and U. Erez, "Comparison of practical feedback algorithms for multiuser MIMO," *IEEE Trans. Commun.*, vol. 58, no. 8, pp. 2436–2446, Aug. 2010.
[5] W.Wang, G. Durisi, T. Koch, and Y. Polyanskiy, "Diversity versus channel knowledge at finite block-length," in *Proc. of the 2012 IEEE Information Theory Workshop*, Sep. 2012, pp. 572–576.
[6] C. Tian, J. Chen, S. N. Diggavi, and S. Shamai, "Optimality and approximate optimality of source-channel separation in networks," *IEEE Trans. Inf. Theory*, vol. 60, no. 2, pp. 904–918, Feb. 2014.
[7] D. Gunduz, E. Erkip, A. Goldsmith, and V. Poor, "Source and channel coding for correlated sources over multiuser channels," *IEEE Trans. Inf. Theory*, vol. 55, no. 9, pp. 3927–3944, Sep 2009.
[8] A. Lapidoth and S.Tingueley, "Sending a bivariate Gaussian over a Gaussian MAC," *IEEE Trans. Inf. Theory*, vol. 56, no. 6, pp. 2714–2752, Jun. 2010.
[9] M. Gastpar, "Uncoded transmission is exactly optimal for a simple Gaussian sensor network," *IEEE Trans. Inf. Theory*, vol. 54, no. 11, pp. 5247–5251, Nov. 2008.
[10] C. E. Shannon, "Communication in the presence of noise," *Proceedings of the IRE*, vol. 37, no. 1, pp. 20–21, 1949.
[11] V. Kotel'nikov, *The theory of optimum noise immunity*. New York: McGraw-Hill, 1959.
[12] O. Fresnedo, F. J. Vazquez-Araujo, J. Garcia-Frias, M. Gonzalez-Lopez, and L. Castedo, "Comparison between analog joint source-channel coded and digital BICM systems," in *Proc. of the IEEE International Conference on Communications (ICC)*, Jun. 2011.
[13] O. Fresnedo, F. Vzquez-Arajo, P. Surez-Casal, and L. Castedo, "Performance comparison between analog JSCC and digital schemes over MIMO channels," in *Proc. of the XXXIII Simposium Nacional de la Unin Cientfica Internacional de Radio (URSI)*, Sep. 2018.
[14] S. Yao and M. Skoglund, "Analog network coding mappings in Gaussian multiple-access relay channels," *IEEE Trans. Commun.*, vol. 58, no. 7, pp. 1973–1983, Jul. 2010.
[15] V. A. Vaishampayan and S. I. R. Costa, "Curves on a sphere, shift-map dynamics, and error control for continuous alphabet sources," *IEEE Trans. Inf. Theory*, vol. 49, no. 7, pp. 1658–1672, Jul. 2003.
[16] 3GPP, "TS 36.213 v14.2.0: E-UTRA; Physical layer procedures," Tech. Rep.